Journal of Integrative Neuroscience

J. Integr. Neurosci. **2026**; 25(9): 53811
https://doi.org/10.31083/JIN53811

Short Communication

Resting-EEG Characteristics and Classification Model Exploration for Tap Test Prediction in Communicating Hydrocephalus: A Small-Sample Pilot Study

Nan Bai[1,†], Zijia Guo[2,†], Wenxuan Xin[2], Maosheng Xiang[1], Junhao Zhu[1], Yuanming Geng[1], Weiyi Xie[2], Chiyuan Ma[1,2,*]

[1]Department of Neurosurgery, Nanjing Jinling Hospital, Affiliated Hospital of Medical School, Nanjing University, 210093 Nanjing, Jiangsu, China
[2]Jinling Clinical Medical College, Nanjing University of Chinese Medicine, 210023 Nanjing, Jiangsu, China
*Correspondence: machiyuan_nju@126.com (Chiyuan Ma)
[†]These authors contributed equally.
Academic Editor: Bettina Platt
Submitted: 3 February 2026 Revised: 9 June 2026 Accepted: 17 June 2026 Published: 21 September 2026

Abstract

Background: Communicating hydrocephalus is characterized by gait disturbance, cognitive impairment, and altered consciousness. The cerebrospinal fluid (CSF) tap test is widely used to predict shunt responsiveness; however, objective neurophysiological markers are still lacking. Resting-state electroencephalography (RS-EEG) may offer insights into brain network function. **Methods:** Thirty patients with communicating hydrocephalus underwent 19-channel RS-EEG before the CSF tap test. Multimodal EEG features were extracted from 2-second epochs, including spectral power, functional connectivity (coherence and phase-locking value), and nonlinear measures (approximate entropy, Hjorth parameters), then aggregated to subject-level representations. Group differences were explored via correlation with clinical scales, source-level phase transfer entropy, and t-distributed Stochastic Neighbor Embedding (t-SNE) visualization. For classification, logistic regression, linear support vector machine (SVM), and a deep neural network (fully connected or 1D Convolutional Neural Network [1D-CNN]) were trained and compared under nested leave-one-subject-out cross-validation with within-fold feature selection. Model performance was assessed using the area under the receiver operating characteristic curve (AUC), permutation tests, bootstrap 95% confidence intervals, and DeLong tests. **Results:** Responders showed higher alpha-band power, which correlated with Coma Recovery Scale-Revised (CRS-R) improvement ($r = -0.764$, $p = 0.0004$) but not Mini-Mental State Examination (MMSE). Functional connectivity and source-level analyses showed descriptive trends that did not survive false discovery rate correction. t-SNE visualization showed partial separation of responders and non-responders, and EEG data quality did not differ between groups. For classification, linear models matched or exceeded deep learning: in the disorders of consciousness (DOC) subgroup, logistic regression (LR) and SVM achieved an AUC of 0.982 (95% CI: 0.909–1.000) & 0.982 (95% CI: 0.893–1.000) vs. 0.964 (0.84–1.00) for the fully connected network; in the cognitive subgroup, SVM reached an AUC of 0.963 (0.84–1.00), followed by CNN (0.944) and LR (0.926). All models were significant by permutation test ($p < 0.002$). DeLong tests showed no significant difference between deep learning and the best linear model ($p > 0.4$), indicating that EEG features are largely linearly separable. Bootstrap confidence intervals remained above 0.73. **Conclusion:** These findings indicate that EEG-derived spectral features, particularly alpha and theta power, contain linearly separable information related to tap test responsiveness. Linear machine learning models performed on par with deep learning, underscoring the robustness of the neural signal and cautioning against unnecessary model complexity in small clinical samples. This exploratory analysis demonstrates the feasibility of EEG-based prediction but requires prospective external validation.

Keywords: hydrocephalus; electroencephalography; machine learning; deep learning; cerebrospinal fluid; consciousness disorders; cognitive dysfunction

1. Introduction

Communicating hydrocephalus includes idiopathic normal pressure hydrocephalus (iNPH) and secondary forms caused by trauma, hemorrhage, or infection [1]. Its primary clinical manifestations include gait disturbance, cognitive decline, and urinary dysfunction. Ventriculoperitoneal shunting remains the primary treatment; however, a considerable proportion of patients demonstrate limited postoperative improvement, emphasizing the importance of accurate preoperative evaluation [2].

The cerebrospinal fluid (CSF) tap test is widely used to aid diagnosis and predict shunt responsiveness and is recommended by international guidelines as a key preoperative assessment tool [3,4]. Its mechanism is believed to reflect reversible changes in brain network function [5]. However, current evaluation primarily relies on clinical symptom improvement and lacks objective neurophysiological markers.

Electroencephalography (EEG) records cortical neuronal activity with high temporal resolution and is commonly employed in brain function assessment [6]. Resting-state EEG (RS-EEG) captures intrinsic brain network dy-

namics and has been applied in various neurological disorders [7,8]. In iNPH, previous studies have revealed alterations in EEG rhythms and functional connectivity associated with gait and cognitive impairment [9], suggesting its potential as a biomarker for network dysfunction.

Recent advances in artificial intelligence have enabled the efficient extraction of high-dimensional features from EEG signals. Deep learning models have demonstrated promising performance in EEG-based classification tasks [10,11]. Additionally, EEG complexity measures have been associated with neural integrity and cognitive function [12,13].

In this exploratory pilot study, We systematically compared three classifiers—logistic regression, linear support vector machine (SVM), and a deep neural network—with the goal of determining whether complex architectures provide additional benefit over simpler linear models in this small-sample setting.

2. Materials and Methods

2.1 Participants

Thirty patients with communicating hydrocephalus admitted between March 2024 and November 2024 were prospectively enrolled. This was a pilot study without formal sample-size calculation; the sample size was determined by feasibility within the recruitment period (**Supplementary STROBE Checklist**).

The inclusion criteria were as follows: (1) diagnosis of communicating hydrocephalus according to established criteria [2]; (2) ventriculomegaly, defined by an Evans index ≥0.3; and (3) the presence of at least one of the following clinical symptoms: gait disturbance, cognitive impairment, or urinary dysfunction [14]. Exclusion criteria included severe neurological comorbidities that could significantly confound EEG signals or incomplete or poor-quality EEG data.

The CSF tap test was performed by removing 30–50 mL of cerebrospinal fluid via lumbar puncture. CSF tap test responsiveness was defined according to established guidelines [3,4] as a clinically meaningful improvement following cerebrospinal fluid removal. Specifically, responders were identified based on either a ≥2-point increase in the Coma Recovery Scale-Revised (CRS-R) for patients with disorders of consciousness or a ≥4-point increase in the Mini-Mental State Examination (MMSE) for patients with cognitive impairment (**Supplementary Fig. 1**). Clinical assessments were performed within 24–72 hours after the procedure.

2.2 EEG Acquisition and Preprocessing

RS-EEG was recorded using a 19-channel 10–20 system (sampling rate: 500 Hz) during eyes-closed resting state for 5 minutes. Preprocessing followed International Federation of Clinical Neurophysiology (IFCN) recommendations [15], including band-pass filtering (0.1–45 Hz) and independent component analysis for artifact removal. Data were segmented into 2-second epochs. Processing was performed using EEGLAB 2023.0 (Swartz Center for Computational Neuroscience, University of California San Diego, La Jolla, CA, USA) [16]. EEG data were first visually inspected to remove segments contaminated by obvious artifacts. Automated rejection was subsequently applied based on abnormal amplitude and signal fluctuations (Amplitude threshold: ±150 μV; Joint probability: 3 standard deviations; Kurtosis: 3 standard deviations). Independent component analysis was then used to identify and remove artifact-related components, such as eye movements and muscle activity. Only artifact-free epochs were retained for subsequent analysis. The proportion of rejected epochs was calculated for each participant as an indicator of data quality. No subjects were excluded due to missing EEG data; all had sufficient artifact-free epochs after preprocessing.

2.3 Feature Exploration

To comprehensively characterize EEG differences between responders and non-responders, we employed four complementary analytical approaches:

Spectral features were computed as relative power within the δ, θ, α, and β frequency bands [15]. In addition, a spectral covariance matrix was calculated for descriptive visualization of group-level spectral relationships. Specifically, for each 2-second EEG epoch, the power spectral density was estimated using Welch's method, and the spectral covariance matrix was computed as the covariance of the log-transformed spectral power across channels and frequency bins. Functional connectivity was quantified using coherence and phase-locking value (PLV) [17]. For group-level comparisons of functional connectivity edges, the false discovery rate (FDR; Benjamini-Hochberg) was applied to control for multiple testing. Corrected significance was set at $q < 0.05$. Uncorrected results are reported as descriptive trends only.

Source-level features were reconstructed using standardized low-resolution brain electromagnetic tomography (sLORETA) [18], as implemented in Brainstorm3.4 (University of Southern California, Los Angeles, CA, USA) [19], followed by estimation of phase transfer entropy to characterize directed information flow between brain regions.

To reduce redundancy prior to t-distributed Stochastic Neighbor Embedding (t-SNE) visualization, principal component analysis (PCA) was applied strictly within each leave-one-subject-out (LOSO) training fold. Specifically, the PCA transformation matrix was estimated on the training subjects only and then applied to the held-out test subject. This prevents any information leakage from the test set into the visualization [20].

2.4 Model Construction

Three classifiers were evaluated: L2-regularized logistic regression (LR), linear SVM, and a deep neural net-

work. Input features for the disorders of consciousness (DOC) subgroup consisted of absolute log-transformed bandpower (theta, alpha, beta); for the cognitive impairment subgroup, relative bandpower (theta, alpha) was supplemented with nonlinear measures (approximate entropy, Hjorth parameters). The deep network was a fully connected network (DOC) or a 1D Convolutional Neural Network (1D-CNN) with one convolutional layers (cognitive impairment (**Supplementary Fig. 2**)).

A strict LOSO scheme was employed. In each fold, one subject's data were held out for testing. Feature selection was performed using a two-sample *t*-test on each feature within the training set. The top K features with the smallest *p*-values were retained, where K = min (10, total number of features) to balance dimensionality reduction and information retention. All preprocessing (standardization) and hyperparameter tuning (inner Leave-One-Out Cross-Validation [LOOCV] for LR) were conducted within the training set. Subject-level probabilities were obtained by log-odds pooling of the test subject's epoch-level predictions to avoid within-subject dependence.

Model performance was assessed using the area under the receiver operating characteristic curve (AUC), sensitivity, specificity, and accuracy at the subject level. To evaluate statistical significance, we performed a subject-stratified permutation test (5000 iterations) and computed 95% bootstrap confidence intervals (2000 resamples). The DeLong test was used to compare AUCs between models. Calibration was assessed with the Brier score and calibration curves.

No sensitivity analysis was performed because all models within each subgroup used identical feature sets, ensuring fair within-subgroup comparisons. The inclusion of LR and SVM baselines served as internal validation.

3. Results

3.1 Patient Characteristics

A total of 30 patients with communicating hydrocephalus were enrolled, comprising 20 cases of secondary hydrocephalus and 10 cases of idiopathic hydrocephalus (baseline characteristics are provided in **Supplementary Table 1**).

Patients were stratified by clinical status into a DOC group, assessed using the CRS-R, and a cognitive impairment group, assessed using the MMSE.

Based on CSF tap test outcomes, patients were further classified into responders (ΔCRS-R $\geq$2 or ΔMMSE $\geq$4) and non-responders (ΔCRS-R <2 and ΔMMSE <4) (Patient characteristics by group are provided in **Supplementary Table 2**).

The distribution of etiologies (idiopathic vs. secondary) within each subgroup is detailed in **Supplementary Table 2**. Briefly, the DOC subgroup comprised 17 secondary cases; the cognitive subgroup comprised 10 idiopathic and 3 secondary cases.

3.2 Differences in EEG Features

Spectral analysis revealed distinct rhythmic patterns across subgroups. Patients with disorders of consciousness predominantly displayed theta-band activity, whereas those with cognitive impairment demonstrated relatively preserved alpha-band activity.

Compared with non-responders, responders showed a trend toward increased alpha-band power (Fig. 1). Exploratory functional connectivity analysis revealed group-level differences in the alpha band, primarily in the right temporal and occipital regions; however, none of these differences survived FDR correction (all q > 0.05). Accordingly, they are reported as descriptive observations only.

Correlation analysis indicated that EEG-derived features were associated with clinical improvement, as reflected by a strong negative association with CRS-R change scores (r = –0.764, p = 0.0004). This relationship was not observed for MMSE scores, which may reflect differences in sensitivity between clinical scales or underlying neural mechanisms (**Supplementary Fig. 3**).

At the source level, phase transfer entropy analysis revealed regional differences in information flow within theta and alpha bands, but these differences did not reach statistical significance. Given the limited spatial resolution of 19-channel EEG, source estimates are underdetermined; hence, these findings are exploratory.

t-SNE visualization revealed a partial separation between responders and non-responders in the feature space, suggesting distinct differences in EEG-derived representations (Fig. 2).

No significant differences in the rejected epoch ratio were observed between responders and non-responders in either subgroup (**Supplementary Table 3**), suggesting that the observed group differences were unlikely to be driven by variations in EEG data quality.

3.3 Model Performance

Logistic regression and linear SVM both achieved an AUC of 0.982 (95% CI: 0.893–1.00), with perfect accuracy, sensitivity (100%), and specificity (LR: 94%, SVM: 88%). The fully connected network attained an AUC of 0.964 (95% CI: 0.84–1.00) (Fig. 3B). Permutation tests confirmed that all models performed significantly above chance (all p < 0.01). DeLong tests showed no significant difference between the deep network and the linear classifiers (CNN vs. LR: p = 0.48; CNN vs. SVM: p = 0.48). The linear SVM achieved the highest AUC of 0.963 (95% CI: 0.84–1.00), followed by the 1D-CNN (AUC = 0.944, 95% CI: 0.78–1.00) and logistic regression (AUC = 0.926, 95% CI: 0.73–1.00) (Fig. 3C). All permutation tests were significant (p < 0.002). DeLong tests again indicated no significant difference between CNN and the linear models (CNN vs. LR: p = 0.83; CNN vs. SVM: p = 0.82). Detailed performance metrics are presented in Table 1. Notably, no significant difference in baseline Glasgow Coma Scale

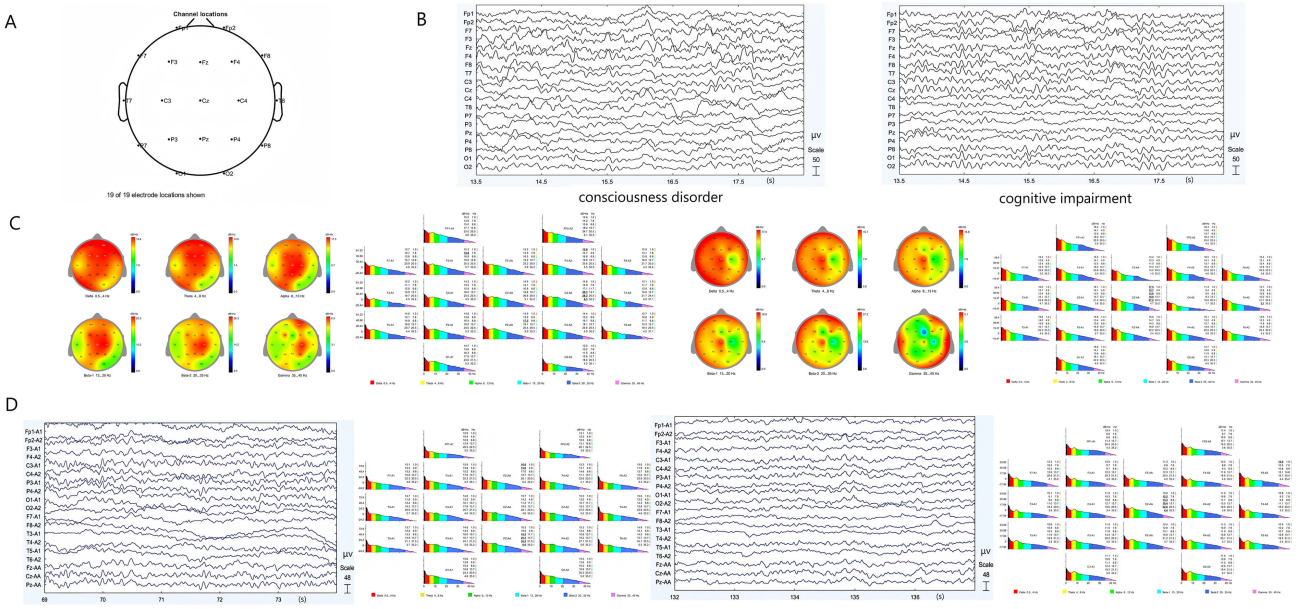

Fig. 1. Rhythmic and spectral characteristics of electroencephalograms in patients with hydrocephalus. (A) Electrode positioning diagram. (B) Raw electroencephalography (EEG) of patients with impaired consciousness and cognitive impairment. (C) Power spectrum and topography (left: cognitive impairment patients; right: consciousness impairment patients). (D) Rhythmic and spectral changes in patients showing significant symptom improvement following the tap test. Fp, frontopolar; C, central; P, parietal; O, occipital; F, frontal; T, temporal; Cz, central midline; A, auricular.

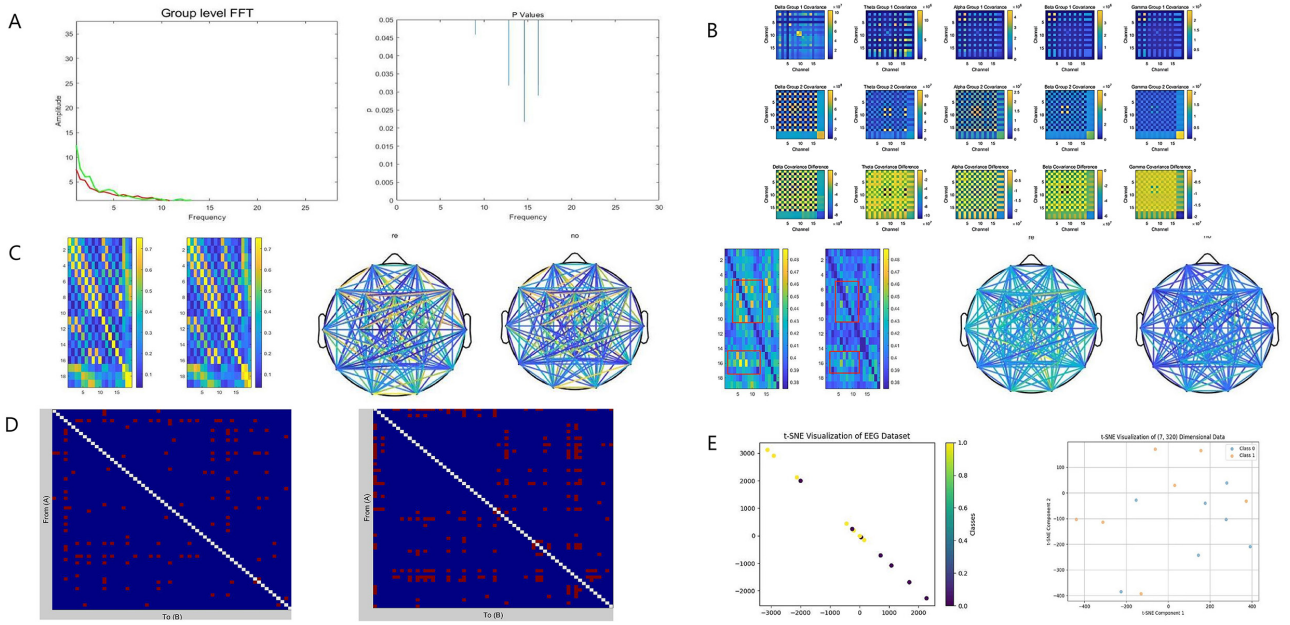

Fig. 2. Differential characteristics of resting-state electroencephalography (RS-EEG) in patients with hydrocephalus showing improvement and no improvement following tap test. (A) Group-level power spectrum analysis. (B) Spectral Covariance Matrix Plot (Group 1: No Improvement Group; Group 2: Improvement Group). (C) Coherence and phase-locking values in the alpha band (left: coherence; right: phase-locking values). (D) After source localization, phase transfer entropy in the theta and alpha bands (left panel: theta band; right panel: alpha band). (E) t-SNE visualization, yellow represents responders and blue/purple represents non-responders. FFT, Fast Fourier Transform; t-SNE, t-distributed Stochastic Neighbor Embedding; re, responders; no, non-responders.

(GCS) scores was observed between responders and non-responders, suggesting that the observed predictive performance was not attributable to differences in initial clinical severity (Fig. 3A).

Table 1. Subject-level classification performance across subgroups.

Subgroup	Model	AUC (95% CI)	Permutation *p*	DeLong *p* (vs. CNN)
Disorders of consciousness	LR	0.982 (0.909–1.000)	0.0004	0.4795
	SVM	0.982 (0.893–1.000)	0.0014	0.4795
	FC	0.964 (0.840–1.000)	0.0010	—
Cognitive impairment	LR	0.926 (0.732–1.000)	0.0004	0.8250
	SVM	0.963 (0.836–1.000)	0.0002	0.8170
	CNN	0.944 (0.778–1.000)	0.0008	—

AUC, area under the receiver operating characteristic curve; CI, bootstrap confidence interval (2000 resamples); DeLong *p*, comparison with CNN; Permutation *p*, subject-stratified label permutation test (5000 iterations); LR, logistic regression; SVM, support vector machine; CNN, Convolutional Neural Network.

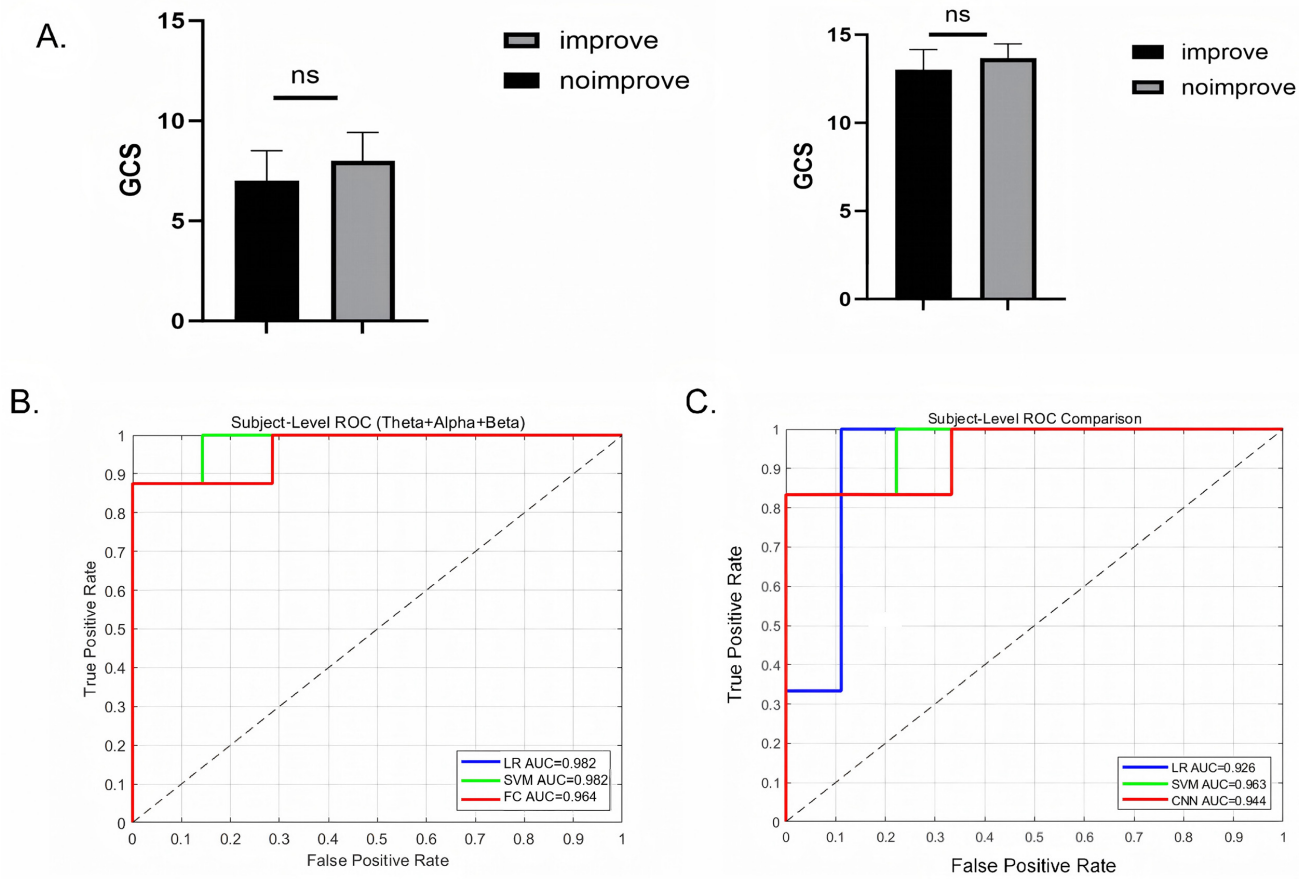

Fig. 3. Communicating hydrocephalus RS-EEG deep learning classification. (A) Baseline Glasgow Coma Scale (GCS) for patients with impaired consciousness (left image) and cognitive impairment (right image). (B) ROC curves for the disorders of consciousness (DOC) subgroup. (C) ROC curves for the cognitive impairment subgroup. ns, not significant; ROC, receiver operating characteristic.

Training dynamics were monitored through loss and accuracy curves (**Supplementary Fig. 3**). The training and validation losses both decreased gradually and plateaued without early divergence. At convergence, the absolute gap between training and validation loss was small (e.g., 0.15 ± 0.05 across folds in the cognitive subgroup). No oscillatory instabilities were observed. Validation loss was evaluated every 10 training iterations; the training curve terminates at the iteration where early stopping was triggered, while the validation curve extends to the final evaluated point. This behavior reflects stable optimization rather than rapid memorization.

4. Discussion

This study examined the association between RS-EEG features and CSF tap test responsiveness in communicating hydrocephalus. The findings suggest that EEG-derived metrics may capture underlying brain network dynamics related to clinical reversibility. Furthermore, the

study population included both idiopathic and secondary hydrocephalus (distribution per subgroup reported in **Supplementary Table 2**). These etiologies may involve distinct pathophysiological mechanisms and baseline network states, which could contribute to variability in EEG features. The small subgroup sizes precluded a stratified analysis by etiology; this remains an important direction for larger future studies.

Theta-dominant activity in patients with impaired consciousness and alpha dominance in cognitively impaired patients may indicate thalamocortical dysregulation [21,22]. Previous studies have shown that oscillatory activity is closely linked to levels of consciousness and cognitive processing [23,24]. Consistent with this, we found that EEG-derived features (primarily alpha power) correlated strongly with improvement on the CRS-R ($r = –0.764$, $p = 0.0004$). In contrast, no significant correlation was observed with MMSE score changes ($r = –0.065$, $p = 0.842$) (**Supplementary Table 4**). This discrepancy suggests that EEG spectral features may be more sensitive to changes in basic arousal and awareness than to higher-order cognitive functions assessed by the MMSE, at least in this patient population.

The observed increase in alpha power among responders may indicate preserved functional reserve and network adaptability. This is consistent with prior iNPH studies reporting EEG rhythm abnormalities and partial reversibility following intervention [8]. EEG complexity has been proposed as a marker of neural integrity, with reduced complexity associated with brain injury severity and impaired recovery [12,13]. Our findings are consistent with this framework.

In both subgroups, linear models (logistic regression and SVM) achieved AUC values comparable to or numerically exceeding those of the deep neural networks: 0.982 (LR/SVM) versus 0.964 (CNN) in the DOC subgroup, and 0.963 (SVM) versus 0.944 (CNN) in the cognitive subgroup. DeLong tests revealed no significant differences between the deep learning and the best linear classifiers ($p > 0.4$ in both subgroups), indicating that EEG features are largely linearly separable and that complex architectures did not yield additional discriminative power. Permutation tests confirmed that the observed AUCs were significantly above chance (all $p < 0.002$). Bootstrap 95% confidence intervals were broad but remained entirely above 0.73, providing further evidence against chance-level performance. These findings suggest that, in small clinical EEG datasets, simple linear models may suffice and offer better interpretability [25]. Nonetheless, the limited sample size precludes definitive conclusions, and external validation in independent cohorts remains essential.

Importantly, no significant differences in EEG data quality, as measured by rejected epoch ratio, were found between responders and non-responders (**Supplementary Table 3**). This reduces the likelihood that the observed classification performance was influenced by systematic differences in signal quality or artifact burden.

Limitations

Several limitations should be acknowledged. The small sample (30 subjects) led to wide bootstrap confidence intervals, but the comparable performance of linear and deep models suggests that overfitting is unlikely to fully explain the high AUCs [26]. This was a single-center study, and site-specific factors may influence generalizability. External validation in independent cohorts is lacking, and the modest calibration slopes indicate that predicted probabilities should be interpreted cautiously. Additionally, the inclusion of both idiopathic and secondary hydrocephalus may have introduced etiological heterogeneity that could influence EEG features and model generalizability. Future multicenter studies with prospective validation are needed to confirm these exploratory findings and should include linear baselines as a standard benchmark.

5. Conclusions

In conclusion, resting-state EEG features may reflect brain network alterations associated with cerebrospinal fluid tap test responsiveness in communicating hydrocephalus. Although the proposed multimodal approach shows preliminary potential, the results should be interpreted with caution, given the small sample size and the possibility of overfitting.

Availability of Data and Materials

The datasets generated and analyzed during the current study are not publicly available due to restrictions imposed by the institutional ethics committee and the need to protect participant privacy and confidentiality. However, the data may be made available from the corresponding author upon reasonable request, subject to approval by the relevant ethics committee and completion of a data-sharing agreement.

Author Contributions

CM conceived and designed the study. ZG, WXin, MX, JZ, YG, WXie, and CM contributed to the literature search for the article and the conceptualization of the study. NB and ZG drafted the article. WXin, MX, JZ, YG, and WXie critically reviewed and revised the article. NB drew the figure. All authors contributed to editorial changes in the manuscript. All authors read and approved the final manuscript. All authors have participated sufficiently in the work and agreed to be accountable for all aspects of the work.

Ethics Approval and Consent to Participate

The study was conducted in accordance with the Declaration of Helsinki and approved by the Ethics Commit-

tee of Nanjing Jinling Hospital, Nanjing University, approval number: 2024DZKY-060-01. All participants provided written informed consent.

Acknowledgment

Not applicable.

Funding

This research was funded by the Jiangsu Provincial Department of Science and Technology (BE2022821) and Project of Jiangsu Science and Technology Plan (BK20243058).

Conflicts of Interest

The authors declare no conflicts of interest.

Supplementary Material

Supplementary material associated with this article can be found, in the online version, at https://doi.org/10.31083/JIN53811.

References

[1] Karimy JK, Reeves BC, Damisah E, Duy PQ, Antwi P, David W, et al. Inflammation in acquired hydrocephalus: pathogenic mechanisms and therapeutic targets. Nature reviews. Neurology. 2020; 16: 285–296. https://doi.org/10.1038/s41582-020-0321-y

[2] Espay AJ, Da Prat GA, Dwivedi AK, Rodriguez-Porcel F, Vaughan JE, Rosso M, et al. Deconstructing normal pressure hydrocephalus: Ventriculomegaly as early sign of neurodegeneration. Annals of Neurology. 2017; 82: 503–513. https://doi.org/10.1002/ana.25046

[3] Nakajima M, Yamada S, Miyajima M, Ishii K, Kuriyama N, Kazui H, et al. Guidelines for Management of Idiopathic Normal Pressure Hydrocephalus (Third Edition): Endorsed by the Japanese Society of Normal Pressure Hydrocephalus. Neurologia Medico-chirurgica. 2021; 61: 63–97. https://doi.org/10.2176/nmc.st.2020-0292

[4] Relkin N, Marmarou A, Klinge P, Bergsneider M, Black PM. Diagnosing idiopathic normal-pressure hydrocephalus. Neurosurgery. 2005; 57: S4–S16; discussion ii–v. https://doi.org/10.1227/01.neu.0000168185.29659.c5

[5] Griffa A, Bommarito G, Assal F, Herrmann FR, Van De Ville D, Allali G. Dynamic functional networks in idiopathic normal pressure hydrocephalus: Alterations and reversibility by CSF tap test. Human Brain Mapping. 2021; 42: 1485–1502. https://doi.org/10.1002/hbm.25308

[6] Hallett M, DelRosso LM, Elble R, Ferri R, Horak FB, Lehericy S, et al. Evaluation of movement and brain activity. Clinical Neurophysiology: Official Journal of the International Federation of Clinical Neurophysiology. 2021; 132: 2608–2638. https://doi.org/10.1016/j.clinph.2021.04.023

[7] Zhang C, Cong F, Kujala T, Liu W, Liu J, Parviainen T, et al. Network Entropy for the Sequence Analysis of Functional Connectivity Graphs of the Brain. Entropy (Basel, Switzerland). 2018; 20: 311. https://doi.org/10.3390/e20050311

[8] Aoki Y, Kazui H, Pascual-Marqui RD, Ishii R, Yoshiyama K, Kanemoto H, et al. EEG Resting-State Networks Responsible for Gait Disturbance Features in Idiopathic Normal Pressure Hydrocephalus. Clinical EEG and Neuroscience. 2019; 50: 210–218. https://doi.org/10.1177/1550059418812156

[9] Seo JG, Kang K, Jung JY, Park SP, Lee MG, Lee HW, et al. Idiopathic normal pressure hydrocephalus, quantitative EEG findings, and the cerebrospinal fluid tap test: a pilot study. Journal of clinical neurophysiology : official publication of the American Electroencephalographic Society. 2014; 31: 594–599. https://doi.org/10.1097/WNP.0000000000000105

[10] Klepl D, He F, Wu M, Blackburn DJ, Sarrigiannis P. EEG-Based Graph Neural Network Classification of Alzheimer's Disease: An Empirical Evaluation of Functional Connectivity Methods. IEEE Transactions on Neural Systems and Rehabilitation Engineering: a Publication of the IEEE Engineering in Medicine and Biology Society. 2022; 30: 2651–2660. https://doi.org/10.1109/TNSRE.2022.3204913

[11] Craik A, He Y, Contreras-Vidal JL. Deep learning for electroencephalogram (EEG) classification tasks: a review. Journal of Neural Engineering. 2019; 16: 031001. https://doi.org/10.1088/1741-2552/ab0ab5

[12] Ren Z, Yue M, Han X, Zhao Z, Wang B, Hong Y, et al. The potential of the Lempel-Ziv complexity of the EEG in diagnosing cognitive impairment in patients with temporal lobe epilepsy. Epileptic Disorders: International Epilepsy Journal with Videotape. 2023; 25: 331–342. https://doi.org/10.1002/epd2.20044

[13] Alkhachroum A, Fló E, Manolovitz B, Cohan H, Shammassian B, Bass D, et al. Resting-State EEG Signature of Early Consciousness Recovery in Comatose Patients with Traumatic Brain Injury. Neurocritical Care. 2024; 41: 855–865. https://doi.org/10.1007/s12028-024-02005-2

[14] Saito M, Nishio Y, Kanno S, Uchiyama M, Hayashi A, Takagi M, et al. Cognitive profile of idiopathic normal pressure hydrocephalus. Dementia and Geriatric Cognitive Disorders Extra. 2011; 1: 202–211. https://doi.org/10.1159/000328924

[15] Babiloni C, Barry RJ, Başar E, Blinowska KJ, Cichocki A, Drinkenburg WHIM, et al. International Federation of Clinical Neurophysiology (IFCN) - EEG research workgroup: Recommendations on frequency and topographic analysis of resting state EEG rhythms. Part 1: Applications in clinical research studies. Clinical Neurophysiology: Official Journal of the International Federation of Clinical Neurophysiology. 2020; 131: 285–307. https://doi.org/10.1016/j.clinph.2019.06.234

[16] Delorme A, Makeig S. EEGLAB: an open source toolbox for analysis of single-trial EEG dynamics including independent component analysis. Journal of Neuroscience Methods. 2004; 134: 9–21. https://doi.org/10.1016/j.jneumeth.2003.10.009

[17] van der Wijk G, Blaskovich B, Farahzadi Y, Simor P. Unaltered EEG spectral power and functional connectivity in REM microstates in frequent nightmare recallers: are nightmares really a REM parasomnia? Sleep Medicine. 2020; 75: 192–200. https://doi.org/10.1016/j.sleep.2020.07.014

[18] Pascual-Marqui RD. Standardized low-resolution brain electromagnetic tomography (sLORETA): technical details. Methods and Findings in Experimental and Clinical Pharmacology. 2002; 24: 5–12.

[19] Tadel F, Baillet S, Mosher JC, Pantazis D, Leahy RM. Brainstorm: a user-friendly application for MEG/EEG analysis. Computational Intelligence and Neuroscience. 2011; 2011: 879716. https://doi.org/10.1155/2011/879716

[20] Varoquaux G, Cheplygina V. Machine learning for medical imaging: methodological failures and recommendations for the future. NPJ digital medicine. 2022; 5: 48. https://doi.org/10.1038/s41746-022-00592-y

[21] Schiff ND. Central thalamic contributions to arousal regulation and neurological disorders of consciousness. Annals of the New York Academy of Sciences. 2008; 1129: 105–118. https://doi.org/10.1196/annals.1417.029

[22] Edlow BL, Claassen J, Schiff ND, Greer DM. Recovery from disorders of consciousness: mechanisms, prognosis and emerg-

ing therapies. Nature Reviews. Neurology. 2021; 17: 135–156. https://doi.org/10.1038/s41582-020-00428-x

[23] Brown EN, Lydic R, Schiff ND. General anesthesia, sleep, and coma. The New England Journal of Medicine. 2010; 363: 2638–2650. https://doi.org/10.1056/NEJMra0808281

[24] Purdon PL, Pierce ET, Mukamel EA, Prerau MJ, Walsh JL, Wong KFK, et al. Electroencephalogram signatures of loss and recovery of consciousness from propofol. Proceedings of the National Academy of Sciences of the United States of America. 2013; 110: E1142–E1151. https://doi.org/10.1073/pnas.1221180110

[25] Bomatter P, Paillard J, Garces P, Hipp J, Engemann DA. Machine learning of brain-specific biomarkers from EEG. EBioMedicine. 2024; 106: 105259. https://doi.org/10.1016/j.ebiom.2024.105259

[26] Pahwa B, Tayal A, Shukla A, Soni U, Gupta N, Bassey E, et al. Utility of Machine Learning in the Management of Normal Pressure Hydrocephalus: A Systematic Review. World Neurosurgery. 2023; 177: e480–e492. https://doi.org/10.1016/j.wneu.2023.06.080